Control of platelet CLEC-2-mediated activation by receptor clustering and tyrosine kinase signalling

Article

Martyanov, A. A., Balabin, F. A., Dunster, J. L. ORCID: https://orcid.org/0000-0001-8986-4902, Panteleev, M. A., Gibbins, J. M. ORCID: https://orcid.org/0000-0002-0372-5352 and Sveshnikov, A. N. (2020) Control of platelet CLEC-2-mediated activation by receptor clustering and tyrosine kinase signalling. Biophysical Journal, 118 (11). ISSN 0006-3495 doi: 10.1016/j.bpj.2020.04.023 Available at https://centaur.reading.ac.uk/90007/

It is advisable to refer to the publisher's version if you intend to cite from the work. See Guidance on citing.
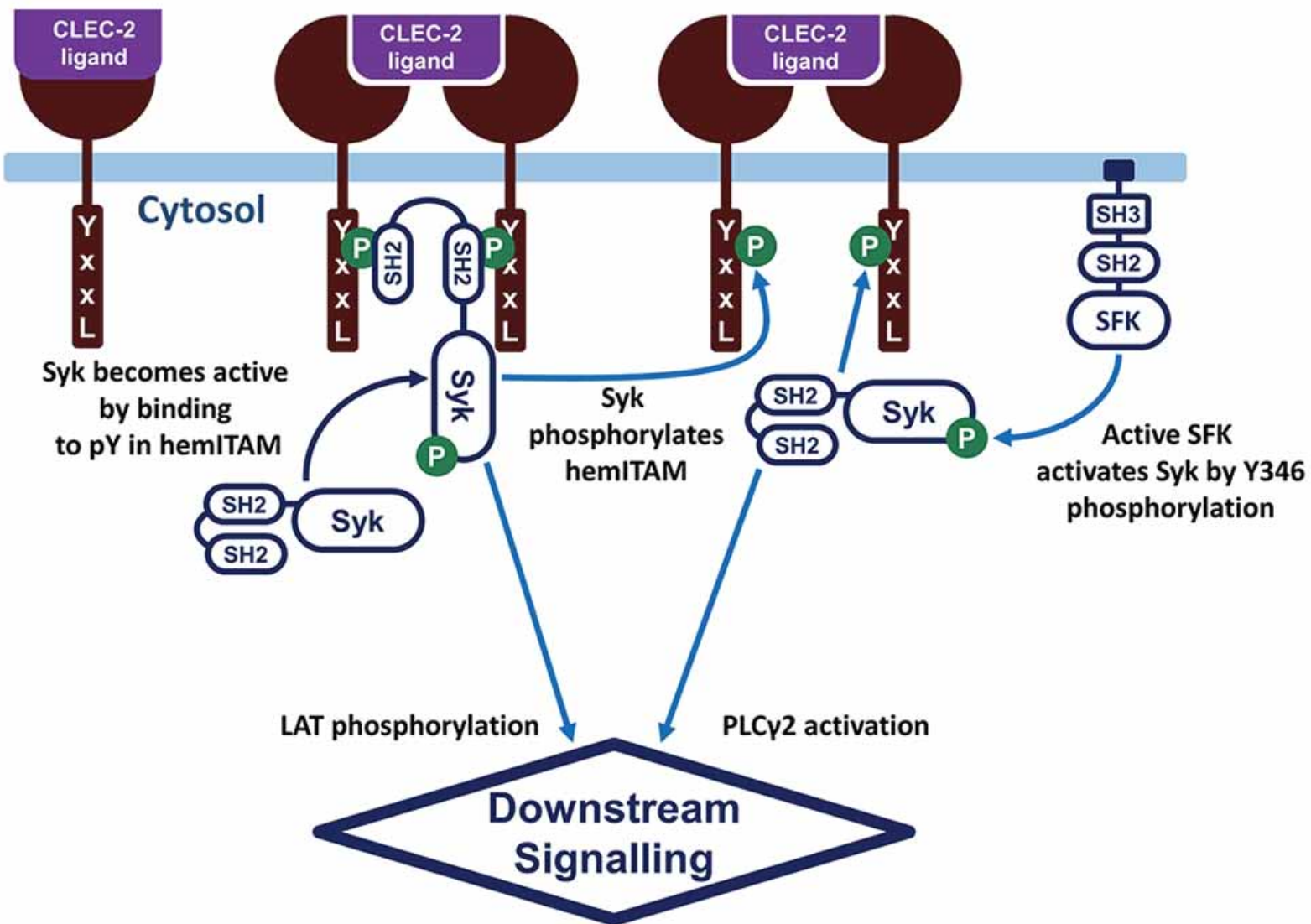
To link to this article DOI: http://dx.doi.org/10.1016/j.bpj.2020.04.023

www.reading.ac.uk/centaur

CentAUR

Central Archive at the University of Reading

Reading's research outputs online

CLEC-2 ligand

Cytosol

Syk becomes active by binding to pY in hemITAM

Syk phosphorylates hemITAM

Active SFK activates Syk by Y346 phosphorylation

LAT phosphorylation

PLCγ2 activation

Downstream Signalling

A

$$\frac{dC^*}{dt} = -k_1 C^* C^{Clust} - 2k_2 C^* C^* + k_{-1} s C^{Clust}$$

$$\frac{dC^{Clust}}{dt} = 2k_2 C^* C^* - k_{-2} C^{Clust} C^{Clust} + k_3 C^{Clust}$$

k_2 Clustering

k_{-2} Clustering

k_1 Clustering

k_{-1} Clustering

k_3 Clustering

Plasma Membrane

CLEC-2 monomer

Phosphate

CLEC-2 Ligand

"CLEC-2 clustering" module

B "Quiescent state" module

CD148

SH3 SH2 SFK

Csk Csk

SH2 SH2 Syk

SH2 SH2 Syk

SH2 Syk

Cytosol

C

Cytosol

TULA-2

TULA-2

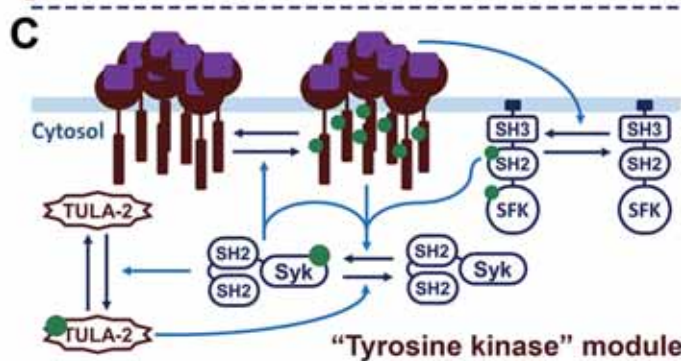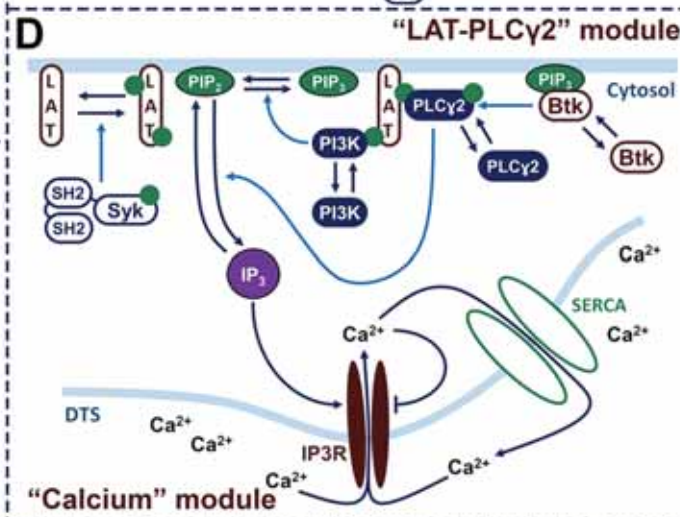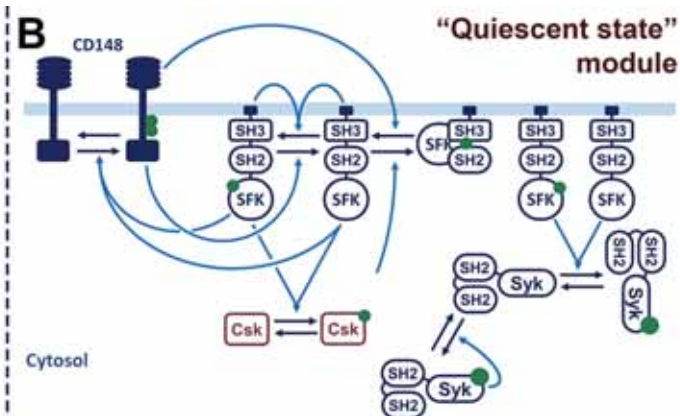SH2 SH2 Syk

SH2 SH2 Syk

SH3 SH2 SFK

SH3 SFK

"Tyrosine kinase" module

D "LAT-PLCγ2" module

LAT LAT PIP$_2$ PIP$_3$ LAT PLCγ2 PIP$_2$ Btk Cytosol

PI3K PLCγ2 Btk

SH2 SH2 Syk PI3K

IP$_3$

Ca^{2+}

SERCA

Ca^{2+}

Ca^{2+}

DTS Ca^{2+} Ca^{2+}

IP3R

Ca^{2+} Ca^{2+}

"Calcium" module

E

Syk Y525 (molecules/platelet) / Blot Intensity vs Time, s

Model — Manne *et. al.* 2013

F

LAT Y191 (molecules/platelet) / Blot Intensity vs Time, s

Model — Manne *et. al.* 2013

G

PLCγ2 Y759 (molecules/platelet) / Blot Intensity vs Time, s

Model — Manne *et. al.* 2013

A

Ca²⁺, μM (y-axis labels for left panels, ranging 0,0 to 1,0)
Time, s

Ligand mediated receptor dimerisation

Post-ligation receptor dimerisation

Cytosol

CLEC-2 Ligand   CLEC-2 monomer

B
CLEC-2 Cluster Size
— Ligand mediated receptor dimerisation
— Post-ligation receptor dimerisation
Time, s

C
Active PLCγ2 molecules
— Ligand mediated receptor dimerisation
— Post-ligation receptor dimerisation
Time, s

D
Ca²⁺, nM
— Ligand mediated receptor dimerisation
— Post-ligation receptor dimerisation
Time, s

A

Sensitivity Score

CLEC-2 Clustering module
- CLEC2 Clustering: k-2
- CLEC2 Clustering: k-1
- CLEC2 Clustering: k1
- CLEC2

Tyrosine-kinase module
- $kcat^{Syk}$
- Km^{Syk}
- $kS1^{SH2}$
- Syk

LAT-PLCγ2 module
- Kr^{LAT}
- $kcat^{Btk}$
- Km^{Btk}
- LAT

B Clustering: k_{-2}

C Clustering: k_{-1}

D Clustering: k_3

E $CLEC-2$

F k_{cat}^{Syk}, s^{-1}

G $Km^{Syk}, \mu M$

H $k_{S1}^{SH2}, s^{-1} \times \mu M^{-1}$

I Syk

J Kr^{LAT}, s^{-1}

K k_{cat}^{Btk}, s^{-1}

L $Km^{Btk}, \mu M$

M LAT

A Vehicle

Fura-RED 405/488 Ratio, a. u.

— Fucoidan, 24°C
— Fucoidan, 37°C

Time, s

B mβCD

Fura-RED 405/488 Ratio, a. u.

— Fucoidan, 24°C
— Fucoidan, 37°C

Time, s

C

Experiment
- 100 µg/ml Fucoidan 25°C
- 100 µg/ml Fucoidan 37°C
- 100 µg/ml Fucoidan 1 mM mβCD
- 5 µg/ml CRP
- mQ

Model
- 100 µg/ml Fucoidan 25°C
- 100 µg/ml Fucoidan 37°C
- 100 µg/ml Fucoidan 1 mM mβCD 25°C

LAT Y191 (molecules/platelet)

Fluorescence intensity, r.u.

Time, s

D

1 µg/ml Fucoidan   10 µg/ml Fucoidan   100 µg/ml Fucoidan

Time (s) 0 15 30 60 90 120 150 180 300

25°C

pY-20

α-Tub

Time (s) 0 15 30 60 90 120 150 180 300

37°C

pY-20

α-Tub

MW (kDa)
150
100
75
50
37
25

E

pY 20, a.u.

■ 25°C
■ 37°C

Time, s

F

pY 20, a.u.

Time, s

G

pY 20, a.u.

Time, s

A

B Platelet — 10 μm

C

D Platelet — 10 μm
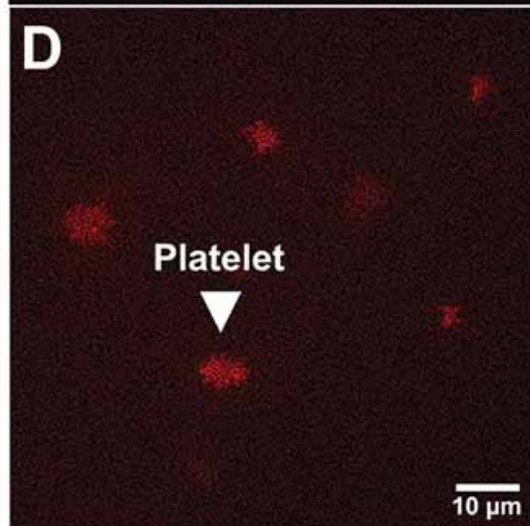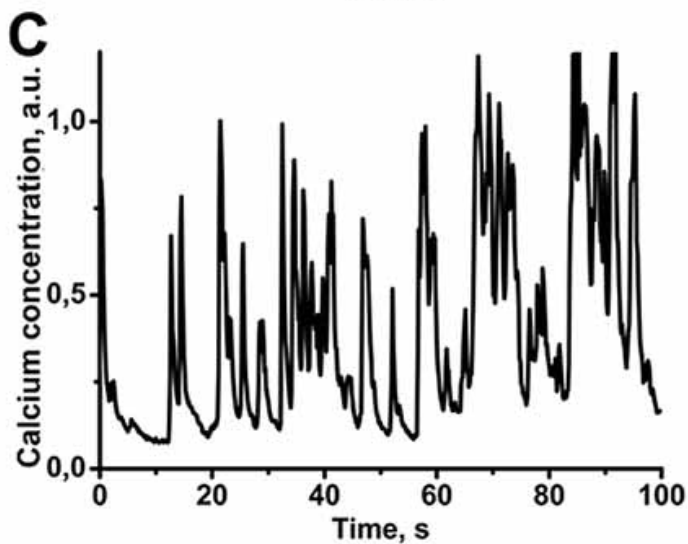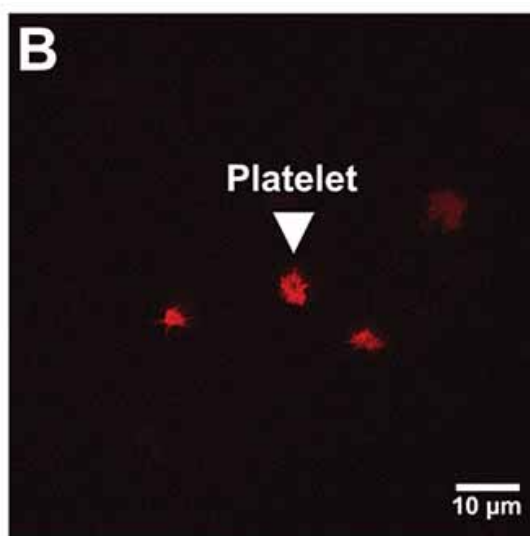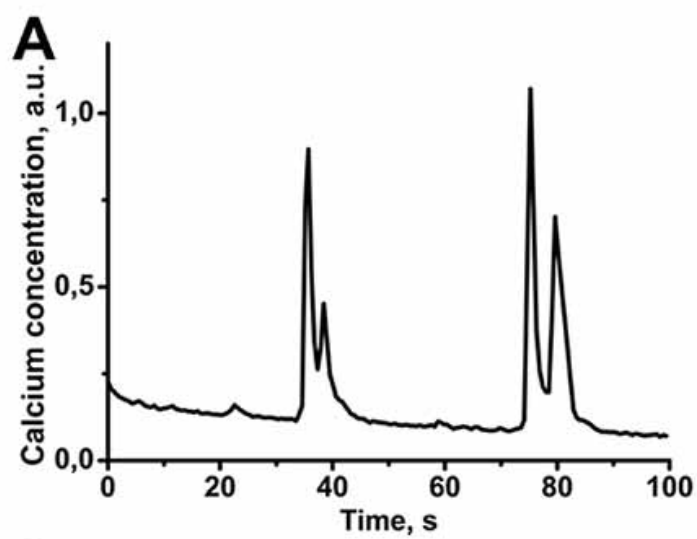
25°C

37°C

E

F

Control of platelet CLEC-2-mediated activation by receptor clustering and tyrosine kinase signalling

A. A. Martyanov, F. A. Balabin, J. L. Dunster, M. A. Panteleev, J. M. Gibbins and A. N. Sveshnikova

Running title: Mechanisms of platelet CLEC-2 activation

Abstract

Platelets are blood cells responsible for vascular integrity preservation. The activation of platelet receptor CLEC-2 could partially mediate the latter function. Although this receptor is considered to be of importance for hemostasis, the rate-limiting steps of CLEC-2 induced platelet activation are not clear. Here we aimed to investigate CLEC-2-induced platelet signal transduction using computational modelling in combination with experimental approaches. We developed a stochastic multicompartmental computational model of CLEC-2 signalling. The model described platelet activation beginning with CLEC-2 receptor clustering, followed by Syk and SFK phosphorylation, determined by the cluster size. Active Syk mediated LAT protein phosphorylation and membrane signalosome formation, which resulted in the activation of Btk, PLC and PI3K, calcium and phosphoinositide signalling. The model parameters were assessed from published experimental data. Flow cytometry, TIRF and confocal microscopy and western blotting quantification of the protein phosphorylation were used for the assessment of the experimental dynamics of CLEC-2-induced platelet activation. Analysis of the model revealed that the CLEC-2 receptor clustering leading to the membrane-based signalosome formation is a critical element required for the accurate description of the experimental data. Both receptor clustering and signalosome formation are among the rate-limiting steps of CLEC-2-mediated platelet activation. In agreement with these predictions, the CLEC-2 induced platelet activation, but not activation mediated by G-protein coupled receptors, was strongly dependent on temperature conditions and cholesterol depletion. Besides, the model predicted that CLEC-2 induced platelet activation results in cytosolic calcium spiking, which was confirmed by single platelet TIRF microscopy imaging. Our results suggest a refined picture of the platelet signal transduction network associated with CLEC-2. We show that the tyrosine kinases activation is not the only rate-limiting step in CLEC-2 induced activation of platelets. Translocation of receptor-agonist complexes to the signalling region and LAT-signalosome formation in this region are limiting CLEC-2-induced activation as well.

Statement of significance

CLEC-2 is a recently discovered platelet receptor implicated in the control of vascular integrity. Here we computationally reconstructed the regulation of tyrosine-kinase and calcium signalling network that controls blood platelet activation via CLEC-2 receptor. We demonstrated that the assembly of the receptors in clusters is the rate-limiting processes in the tyrosine kinase-associated signal transduction, which could explain the slow rates of platelet activation by CLEC-2. Additionally, we demonstrated for the first time that CLEC-2 stimulation leads to cytosolic calcium spiking, with a qualitative change caused by the clustering-affecting influences such as temperature and cholesterol saturation.

1. Introduction

The main task of platelets, non-nucleated cellular fragments produced from megakaryocytes in the bone marrow, is prevention of the blood loss upon vessel wall disruption (1). Platelets circulate in the cardiovascular system for approximately seven days, until they get eliminated in the spleen or liver (2). Alongside their primary role in hemostasis, platelets were demonstrated to be involved in angiogenesis (3), tissue remodelling (4, 5), and leukocyte recruitment under inflammatory conditions (6, 7). Platelets respond gradually to various activators (1). Platelet response to the contact with extracellular matrix

protein collagen includes shape change, granule release and, in some cases, cell death (8). In contrast, platelet response to ADP includes only shape change and integrin activation (8).

There are two main types of signalling pathways in blood platelets, associated either with G-proteins or with tyrosine kinase signalling (9). Platelet G-protein coupled receptors (GPCR) govern responses to ADP (P2Y1, P2Y12 receptors), thromboxane A2 (TxA$_2$), thrombin (protease-activated receptors 1 and 2 (PAR1, PAR4)), epinephrine (α2A) and prostacyclin (IP) (10, 11). Platelet receptors that induce tyrosine kinase network of signalling are the receptors for collagen (glycoprotein VI (GPVI)) (8, 12), for IgG (FcγRIIa) (9), and recently found on platelets receptor CLEC-2 (C-type lectin-like receptor II-type (CLEC-2)) (8). The only confirmed endogenous CLEC-2 ligand is a membrane protein podoplanin, expressed by the lymphatic endothelial cells (13, 14). Therefore the primary platelet CLEC-2 physiological function is considered to be the separation of blood and lymphatic systems (15–18). Other known CLEC-2 agonists are snake venom protein rhodocytin (19, 20), and brown seaweed extract fucoidan (21). CLEC-2 also contributes to the maintenance of blood vessel integrity during inflammatory conditions (17, 22–25) and has a role in thrombus formation and wound healing (7, 23, 26–29) and in various pathologies (30–32). This makes CLEC-2 a prospective therapeutic target (7, 29, 32, 33). Thus, systemic understanding of the CLEC-2 signalling is of essential importance.

A distinct feature observed upon platelet activation via CLEC-2 by either podoplanin, rodocytin or fucoidan was 1-2 minute lag-time before activation (21, 34). This has been demonstrated using spectrofluorimetric assay of platelet cytosolic calcium (21). However, it is not understood, whether platelet CLEC-2 can induce cytosolic calcium spiking, prolonged cytosolic calcium oscillations or transient increase of cytosolic calcium. The prolonged platelet CLEC-2 induced response may be a consequence of ADP-containing granule secretion and TxA2 synthesis. Another possible cause of the significant activation lag-time is the receptor clustering, as was proposed by Pollitt et al. (34). Indeed, glycosylated extracellular stalk regions (35), as well as the GxxG region in the transmembrane domain of CLEC-2 (35, 36), lead to homodimerisation of the recombinant CLEC-2 proteins (35). On the surface of the resting platelets, CLEC-2 is present both in dimeric and monomeric forms (35, 36). Upon ligand binding, CLEC-2 undergoes multimerisation (36), which might be ligand driven (e.g. tetrameric rhodocytin can bind two copies of single CLEC-2, or two CLEC-2 dimers simultaneously (37)). On the other hand, non-multimeric podoplanin still induces CLEC-2 cluster formation (38), which implies more complex clustering mechanisms. The platelet responses to CLEC-2 are also highly dependent on actin polymerisation and cholesterol presence in the plasma membrane (34, 39). However, unlike cholesterol presence, actin cytoskeleton reorganization is not required for CLEC-2 oligomerisation (34). Badolia et al. have recently reported that CLEC-2 induced signalling is still detectable after the abrogation of secondary activation (40).

Computational modelling approach could be useful to reveal the sequence of events in CLEC-2 induced platelet activation and identification of rate-limiting steps in this pathway. Mukherjee et al. demonstrated that receptor clustering is significant for the activation of ITAM-bearing receptors (B-cell receptors (BCR) and T-cell receptors (TCR)) (41). The significance of platelet receptor clustering was demonstrated experimentally for CLEC-2 (38) and GPVI (42), however, the computational models of GPVI-induced platelet activation do not incorporate the receptor clustering (43, 44). Due to their small size, platelets do not possess significant amounts of signalling proteins. For example, there are only 2000 copies of phospholipase Cγ2 (PLCγ2) in platelets (approximately 500 nM). Even upon strong activation, no more than 25% of signalling proteins become active (44). Thus, it can be claimed that there are less than 100 active signal-transducing proteins in platelets upon weak stimulation. Due to low amounts of active participants of the signalling cascades in platelets, deterministic modelling might not be capable of providing reliable calculation results. Thus, stochastic approaches are required for platelet models (45–47).

Here we aimed to reveal the primary events of platelet activation upon stimulation through CLEC-2 by means of computational modelling and experimental analysis. The proposed *in silico* model described platelet activation starting from ligand binding to CLEC-2 and proceeding until calcium ions release from the dense tubular system. The model predicted that besides tyrosine kinase activity, platelet activation via CLEC-2 is limited by the CLEC-2 receptor clustering in the plasma membrane, the CLEC-2 clustering pattern and the LAT signalosome formation. Model predictions were supported experimentally by an essential dependence of CLEC-2-induced platelet activation on temperature and by modulation of membrane saturation of cholesterol by methyl-β-Cyclodextrin (mβCD). The model also predicted CLEC-2 induced calcium spiking, which was confirmed experimentally using total internal reflection microscopy (TIRF-microscopy). Our data enable us to propose a refined concept of signal transduction upon platelet activation via CLEC-2.

2. Methods

Reagents

The sources of the materials were as follows: calcium-sensitive cell-permeable fluorescent dye Fura-2-AM, Fura Red-AM (Molecular Probes, Eugene, OR); Fucoidan from *Fucus vesiculosis*, ADP, PGI$_2$, EGTA, HEPES, bovine serum albumin, apyrase grade VII, methyl-β-cyclodextrin (mβCD) (Sigma-Aldrich, St Louis, MO). VM-64 antibody was a kind gift of Dr A.V. Mazurov (NMRC of Cardiology, Moscow, RF) (48).

Blood collection and platelet isolation

Healthy volunteers, both men and women aged between 18 and 35 years were recruited into the study. Investigations were performed under the Declaration of Helsinki and written informed consent was obtained from all donors. Blood was collected into 4.5 ml tubes containing 3,8% sodium citrate (1:9 vol/vol) and supplemented by apyrase (0.1 U/mL). The study was approved by the Independent Ethics Committee at CTP PCP RAS (1_2018-1 from 12.01.2018). Platelets were purified by double centrifugation as described previously (45, 49). Briefly, platelet-rich plasma was obtained by centrifugation at 100 g for 8 minutes. Platelet-rich plasma was supplemented with additional sodium citrate (27 mM) and centrifuged at 400 g for 5 minutes. The resultant supernatant was removed and platelets resuspended in Tyrode's buffer (150 mM NaCl, 2.7 mM KCl, 1 mM MgCl2, 0.4 mM NaH2PO4, 5 mM HEPES, 5 mM glucose, 0.2% bovine serum albumin, pH 7.4). Alternatively, blood was collected in Li-heparin (IMPROVACUTER®) or hirudin (SARSTEDT Monovette®) containing vacuum tubes.

Flow cytometry and inhibitory analysis

For continuous flow cytometry experiments, washed platelets were incubated with either 2 µM Fura Red-AM (2 µM of Fura-2) before the final wash for 45 minutes at room temperature or for 30 min at 37°C in the presence of apyrase (1 U/mL). Platelets were then incubated in buffer A for 10 minutes and then centrifuged. Whole blood was incubated with either 2 µM Fura Red-AM (or 2 µM of Fluo-3 or Fluo-4 and 2 µM of Fura-2) for 30 min at 37°C in the presence of apyrase (1 U/mL). Whole blood was diluted 20-times with calcium and albumin containing Tyrode's buffer. Samples were diluted to concentration 1000 plt/µl and analysed using FACS Canto II or FACS Aria (BD Biosciences, San Jose, CA, USA) flow cytometer in a continuous regime with 20s interruption for the addition of an activator.

Immunoblotting

Human platelets from drug-free volunteers were prepared on the day of the experiment as described previously (50) and suspended in modified Tyrodes-HEPES buffer (134 mM NaCl, 0.34 mM Na$_2$HPO$_4$, 2.9 mM KCl, 12 mM NaHCO$_3$, 20 mM HEPES, 5 mM glucose, 1 mM MgCl$_2$, pH 7.3) to a density of 1.5×10^9 cells/ml. Stimulation of platelets with 10x fucoidan (final concentration: 1 µg/ml 10 µg/ml, 100 µg/ml), was performed for 0-15-30-60-90-120-150-180-300 s at 25 or 37 °C in an aggregometer with continuous

stirring (1000 rpm). Reactions were abrogated by addition of 4x SDS-PAGE sample treatment buffer (200 mM Tris-HCl pH6.8, b-MeEtOH 400 mM, SDS 4%, Bromphenol blue 0.01%, Glycerol 40%). Samples were then heated to 99°C for 10 minutes and centrifuged at 15000g for 10 minutes in order to remove cell debris.

Proteins were separated by SDS-PAGE on 10% gels and transferred to polyvinylidene difluoride (PVDF) membranes that were then blocked by incubation in 5% (w/v) bovine serum albumin dissolved in TBS-T. Primary and secondary antibodies were diluted in TBS-T containing 2% (w/v) bovine serum albumin and incubated with PVDF membranes for 1.5 h at room temperature. Blots were washed 4 times for 15 minutes in TBS-T after each incubation with antibodies and then developed using an enhanced chemiluminescence detection system using ECL Prime western blotting detection reagent. Primary antibodies were used at a concentration of 1 µg/ml (anti-phosphotyrosine PY20) or diluted 1:1000 (anti-tubulin). Horseradish peroxidase-conjugated secondary antibodies were diluted 1:1000. In order to control for protein loading, membranes were stripped by washing 2 times for 30 minutes in stripping buffer (250 mM Glycine, 0.2% SDS, 0.1% Tween-20, pH 2.2) twice for 10 minutes in PBS and 2 times for 5 minutes in TBST at room temperature. Membranes were then blocked for 30 minutes by 2% TBS-T BSA solution at room temperature and re-stained with anti-tubulin antibodies.

Depletion of platelet cholesterol

Cholesterol was depleted from the plasma membrane of platelets, by incubation of washed platelets for 15 minutes with different concentrations of mβCD at 37° C before stimulation as described in (51).

Immunofluorescent microscopy

Washed human platelets were activated by Fucoidan (100 µg/ml) at 25°C (with or without cholesterol depletion by mβCD) or at 37°C and fixed by 4% PFA after 30, 60, 90, 120, 300 seconds after activation. Platelets incubated with CRP (5 µg/ml) or mQ water for 300s were used as positive and negative controls, correspondingly. Fixed platelets were washed from PFA by sequential centrifugation, resuspended in PBS-BSA buffer and adhered to poly-L-lysine (0.1 % in mQ, Sigma-Aldrich US) covered glass coverslips for 90 minutes at 37°C. Non-adherent platelets were removed by gentle rinsing of the coverslips. Fixed platelets on the glass were then permeabilised by 0.2% Triton X-100 in the presence of 2% BSA and 1% Goat serum. After permeabilisation platelets were incubated with 1:250 diluted LAT pY1911 (Abcam, US) antibodies for 90 minutes at room temperature. After washing primary antibodies off, platelets were incubated with secondary antibodies, conjugated with FITC (Imtek, RF) for 90 minutes in the darkroom at room temperature. After washing off secondary antibodies, cells were additionally fixed by adding 4% PFA for 10 minutes. Samples were then mounted with Dako fluorescence mounting media (Agilent, US). Samples were analyzed by means of Zeiss Axio Observer Z1 microscope (Carl Zeiss, Jena, Germany) in the confocal mode.

Live cell microscopy

For microscopy experiments, platelets were loaded with calcium fluorophores and immobilised by either incubation of platelet suspension in the flow chamber for 5 min, or by perfusing whole blood over the surface at a shear rate of 200 s^{-1} for 5 minutes. For total internal reflection fluorescent (TIRF) microscopy, platelets were immobilised either on fucoidan (100 µg/ml) or anti-CD31 (VM-64) (48) and investigated in flow chambers (52). An inverted Nikon Eclipse Ti-E microscope equipped with 100x/1.49 NA TIRF oil objective was used. Cells were observed in DIC and TIRF modes. 405 nm laser was applied to assess calcium-free Fura-2 fluorescence in a platelet. Calcium concentration was assessed from Fura-2 fluorescence as a ratio of initial and running values with taking exponential bleaching of the dye into account. For temperature fixation, during observation, a lens heater (Bioptechs, Butler, PA) was used.

Data analysis

Nikon NIS-Elements software was used for microscope image acquisition; ImageJ (http://imagej.net/ImageJ) was used for image processing for both TIRF-microscopy and western blotting and microscopy assays from literature. The absolute size of CLEC-2 clusters (Fig. S1D) was calculated from the fluorescence intensity, which was assumed to be proportional to the number of receptors per cluster. It has also been assumed that only CLEC-2 monomers and dimers are present on the surface of resting platelets. Flow cytometry data were processed using FlowJo (http://www.flowjo.com/) software. Statistical analysis was performed in Python 3.6.

Model solution and sensitivity analysis

The model, formed of ordinary differential equations (see supplement) with initial variable values (Table S2, S5, S7) was integrated using the LSODA method in COPASI software. The stochastic model was solved using stochastic integration methods (combined Adaptive SSA/the tau-leap method (53, 54)) implemented in COPASI software, similarly to previously published methods (45, 55). Parameter estimation was performed using Genetic Algorithm. Models are given in the supplement (see Table S9).

Sensitivity score was calculated as $Score = {(O_a - O_i)}/{O_a}$, where O_i and O_a represent the model output (e.g. the steady-state and time to reach the peak in Syk activity) in respect of the initial parameter set (obtained from parameter fitting) and the adapted parameter respectively.

3. Results

3.1. Scheme of biochemical reactions underlying our model of CLEC-2-induced platelet activation.

The model development was carried out based on the known details of the CLEC-2 signalling network. Briefly, after binding of CLEC-2 to its ligand, CLEC-2 receptor-ligand complexes rapidly form tight clusters, predominantly in the lipid rafts (35, 36). Activated and clustered CLEC-2 molecules can be phosphorylated by platelet Syk tyrosine kinases (56). Although it has been proposed that Src family kinases (SFK) also participate in the process of CLEC-2 phosphorylation (57, 58), here in the model we considered SFK merely as a positive mediator for Syk basal activation (17). The inactive Syk rapidly bound two phosphorylated CLEC-2 receptors by two Src homology 2 (SH-2) domains. Association with CLEC-2 resulted in Syk activation and stabilisation of CLEC-2 dimers (17, 59, 60). Binding of SFK to phosphorylated hemITAM also lead to the complete SFK activation, which additionally amplified Syk activation (17, 59). Syk activated T-cell ubiquitin ligand-2 (TULA-2), which is a negative regulator Syk activation (44). Active Syk and SFK phosphorylated an adaptor molecule called linker adapter for T-cells (LAT) leading to LAT-signalosome formation (34, 40, 61), which consists of PLCγ2, phosphoinositide-3-kinase (PI3K), SH2 domain-containing leukocyte phosphoprotein of 76kDa (SLP-76) and a set of other adaptor proteins. In the LAT-signalosome the PI3K became active and produced phosphoinositol-3,4,5 trisphosphate (PIP_3) from phosphoinositol-4,5 bisphosphate (PIP_2) in the surrounding plasma membrane region. The increase in PIP_3 concentration resulted in Bruton's tyrosine kinase (Btk) attraction to the region and phosphorylation and activation of PLCγ2 (62). Finally, PLCγ2 hydrolysed PIP_2 and produced inositol-1,4,5 trisphosphate (IP_3). IP_3 induced Ca^{2+} signalling. A brief scheme of platelet CLEC-2 signalling (Fig. 1) described above was the basis of the constructed computational model.

3.2. Computational model construction

The computational model of CLEC-2 induced platelet activation was designed according to the scheme above. It consisted of 5 compartments: extracellular space, plasma membrane, cytosol, DTS membrane and DTS (Table S1). The model included the following biochemical modules: "CLEC-2 clustering" module, capturing CLEC-2 ligand binding and cluster formation (Tables S2-S4, Fig. 2A); "Quiescent state" module, capturing CD148 and C-terminal Src kinase (Csk) mediated SFK activation and Syk primary activation by active SFKs (Table S5, S6, Fig. 2B); "Tyrosine kinase" module, capturing CLEC-2 phosphorylation and

activation of Syk and SFK kinases (Tables S5, S6, Fig. 2C); "LAT-PLCγ2" module, capturing events downstream of activated Syk and SFK including phosphorylation of LAT, PI3K and Btk incorporation to the signalosome, PLCγ2 activation and production of IP$_3$ (Tables S7, S8, Fig. 2D); "Calcium" module, capturing IP$_3$ induced calcium signalling in platelet cytosol (from (45, 63), Fig. 2D). The underlying systems of differential equations were constructed from current biological knowledge (see above) using the assumptions of either mass action or Henry-Michaelis-Menten kinetics. The probabilities in the corresponding stochastic model were calculated based on the same assumptions. The parameter values were taken from the experimental reports on the corresponding human enzymes, while the numbers of proteins per platelet were taken from the published proteomics data (64). The model reactions, equations and parameter values can be found in Supporting Information.

The "CLEC-2 clustering" module described the process of receptor clustering. Mathematically this description was performed by two differential equations, based on our previously published study (65). This approach was called the "2-equation" model (Fig. 2A). Its applicability and correspondence to an explicit model of receptor cluster formation (called "N-equation" model) and experimental data are given in the Supporting Information (Fig. S1). The "2-equation" model described the behaviour of variables for the concentration of single CLEC-2 molecules and the concentration of CLEC-2 clusters in the plasma membrane (Fig. 2A, S1B). During the estimation of the "CLEC-2 clustering" module parameters, we identified two distinct patterns of receptor clustering in the "2-equation" model. The first, which could be called "ligand-mediated" cluster formation, suggested that the clustering coincides with receptor ligation. The second, called the "post-ligation" cluster formation, suggested that the clusters appear after the formation of receptor-ligand complexes. Both patterns will be discussed further in section 3.3. All of the model calculations were performed with "ligand-mediated" cluster formation model, except where otherwise stated.

For the "Quiescent state" module, the unknown parameters were tuned to obtain 5% of active Syk kinases and 10% of active SFK kinases at the steady-state achieved without CLEC-2 ligand in the system. The CD148 phosphatase and Csk kinase were introduced into the model to maintain this steady-state (Fig. 2B). For the "Tyrosine kinase" module, we assumed that the first event was the phosphorylation of CLEC-2 in clusters by Syk kinases. The activation of Syk kinases, as well as SFK activation, was assumed to occur depending on the CLEC-2 cluster size. The descriptions of the "LAT-PLCγ2" module and the "Calcium" module can be found in the Supporting Information (Fig. 2D). It is noteworthy that the only link between the "Calcium" module and the other modules was the IP$_3$ concentration, which in its turn was mediated by active PLCγ2. That is why we chose the number of active PLCγ2 as one of the major model output. A network diagram depicting all of the reactions and parameters of the model is given in Fig. S2. The corresponding SBML files can be found in the online Supporting Information (also see Table S9 for details).

The full model was constructed as a sum of the separate models described above without further adjustment of the parameters. The full model appeared to be capable of the correct description of the following experimental data. The predicted numbers of active Syk, SFK and the phosphorylated LAT (Fig. 2E, S3, 2F, respectively) were in good agreement with available from experimental literature data (21). However, the predicted numbers of active PLCγ2 described the data less accurately (Fig. 2G), which could be caused by the secondary activation of platelets under the conditions of the experiment.

3.3. Two different clustering patterns predicted by the model

In the process of parameter estimation for "CLEC-2 clustering" module, we identified two different possible sets of parameters, with which the model could describe experimental data from (38) (Fig. 3, S1D). The first observed pattern was called a "ligand-mediated" receptor clustering when the rapid receptor dimerisation immediately followed the receptors' ligation (Fig. 3A). The "ligand-mediated" receptor clustering mode corresponds to the ligand-driven receptor clustering mechanism *in vivo*. The

6

second pattern, when the receptors' ligation did not directly lead to receptor dimerisation, was termed "post-ligation" (Fig. 3A). This mode corresponded to the assumption that CLEC-2 receptor undergoes additional conformational changes after ligation, which made it more prone to clustering. The comparison of the average cluster size between two different schemes is given in Figure 3B. Parameter variation results revealed that the maximum size of the CLEC-2 clusters is determined by the total number of CLEC-2 as well as kinetic parameters of the clustering, both for "ligand-mediated" (Fig. S4A-C) and "post-ligation" (Fig. S4G-L) clustering regimes. However, in the "ligand-mediated" clustering regime, maximum CLEC-2 cluster size appeared to be more sensitive to the assessed parameters, than in the "post-ligation" regime. (Fig. S4).

With both schemes, the full model predicted cytosolic calcium spiking (Fig. 3A). However, the "post-ligation" scheme could not be tuned to induce calcium spiking earlier than 200s after ligand introduction (Fig. 3A,D), despite producing a more significant increase in the number of active PLCγ2 (Fig. 3C) and higher concentration of cytosolic calcium in the cell population (Fig. 3D). However, previous experimental data (21) suggested much shorter activation times for CLEC-2 induced platelet activation, and thus, we preferred the "ligation-mediated" scheme. Curiously, a rapid dimerisation of ITAM receptors was demonstrated to correlate with the shortened cell activation lag-times elsewhere (41).

3.4. Sensitivity analysis of the model

To analyse the influence of unknown parameters and determine the possible rate-limiting steps, we performed a local sensitivity analysis (Fig. 4, S5-S16). Scaled local sensitivities of the time to reach the peak quantities/concentrations of active Syk (S^*), phosphorylated LAT (L^*), active PLCγ2 (p^*), IP$_3$ (I_3), and cytosolic Ca^{2+} to all model parameter values were calculated. The results are given in Figures 4A and S5. Parameters of the "Tyrosine kinase" module had the biggest impact on all of the analysed variables. The "LAT-PLCγ2" module parameters were less influential and "CLEC-2 clustering" module parameters were the least influential. "Tyrosine kinase" module parameters concerning Syk ([Syk]$_0$, k_{cat}^{Syk}, Km^{Syk}, and k_{S1}^{SH2}) influenced all platelet responses, while its parameter for CLEC-2 dephosphorylation rate (Kr^{Phosph}) was the most influential only for S^* (active Syk). Among "LAT-PLCγ2" module, the most influential parameters were the reverse rate of LAT phosphorylation and LAT concentration (Kr^{LAT}, [LAT]$_0$ for all of the variables, except Syk) and the catalytic parameters of Btk kinase (k_{cat}^{Btk}, Km^{Btk}, for all variables except Btk). Finally, among parameters of the "CLEC-2 clustering" module k_{-2}, k_{-1}, k_1 alongside CLEC-2 initial concentration were influential for all responses. Explicit variation of the most influential model parameters for PLCγ2 is given in Figure 4B–M. Variation of the rest of parameters concerning all of the analysed variables and sensitivity scores for all of the variables can be found in Supporting Information (Fig. S6 – S16, Tables S10 – S14, correspondingly). Based on these results we can conclude that the most influential parameters for all of the analysed variables concern Syk kinase activation (k_{S1}^{SH2}, k_{cat}^{Syk}, Km^{Syk}). On the other hand, parameters, governing reverse reactions (Kr^{Phosph}, Kr^{LAT}, Kr^{Syk}) as well as parameters concerning TULA-2 activation (Kf_{Syk}^{TULA2}, Kr_{Syk}^{TULA2}, Kr_{TULA2}^{Syk}) also were among the most influential, which highlights the role of the negative regulators of signalling for CLEC-2 induced platelet activation. Finally, local sensitivity analysis also allowed to identify three rate-limiting reactions: Syk kinase activation, LAT phosphorylation and CLEC-2 cluster formation. Among these reactions, Syk activation was the most influential.

3.5. CLEC-2 agonist fucoidan is capable of evoking calcium response in platelets independently from secondary mediators of signalling

One of the model predictions suggested that CLEC-2 stimulation was sufficient to initiate calcium signalling in platelets (Fig. 3A, D). To test this prediction, we performed flow cytometry experiments on platelets loaded with calcium fluorophore Fura Red (Fig. 5A). To avoid an impact of secondary activation, we pre-incubated platelets with P2Y1 receptor antagonist MRS2179 (Fig. 5A). To assess the predicted

dependence of platelet activation on the clustering of CLEC-2, we investigated the influence of membrane cholesterol content on calcium response. Cholesterol molecules determine the stability of membrane regions, and thus incubation od cells with a cholesterol-binding agent mβCD could disrupt clusters of proteins (51). During experiments, we observed that while high concentrations (5 mM) of mβCD were capable of severe disruption of platelet response to fucoidan (Fig. 5B), relatively low concentrations of mβCD (1 mM) delayed platelet activation not affecting its degree (Fig. 5B). This observation was in agreement with model predictions (Fig. 3D), supporting rapid clustering pattern for CLEC-2 (Fig. 3A). To test the prediction of the model that fucoidan induces rare calcium spiking in platelets instead of a stationary increase in calcium concentration (Fig. 3A), we performed analysis of single-cell calcium signalling using fluorescence microscopy (Fig. 5C,D). Washed Fura Red loaded platelets spread on fucoidan covered glass (Fig. 5C) which resulted in prolonged calcium spiking (Fig. 5D). This observation supported the model prediction that fucoidan is capable of calcium spiking induction.

3.6. Impact of the medium temperature and plasma membrane fluidity on CLEC-2 induced calcium response in platelet suspension

We have performed further investigation of fucoidan-induced intracellular signalling in platelets in the presence of mβCD and temperature variation to test the model predictions on the role of the receptor clustering process. At both room (25°C) and body (37°C) temperature, activation of platelets with fucoidan lead to an increase in cytosolic Ca^{2+} concentration (Fig. 6A). However, at 25°C this increase occurred at 100 s, while at 37 ^{o}C it was significantly more rapid and occurred at 60 s. Pre-incubation of platelets with mβCD further delayed the increase in the concentration of cytosolic calcium both at 25 ^{o}C (240 s) and at 37 ^{o}C (105 s) (Fig. 6B). It should be noted that temperature variation did not affect the activation of platelets by low concentrations (2 μM) of ADP (Fig. S17).

Single-cell analysis by means of immunofluorescent microscopy revealed that at 37°C clustered fractions of phosphorylated LAT, which are known markers of cholesterol-enriched microdomains in platelet membrane (34), appeared at the 30s and the amount of phosphorylated LAT reached its maximal values by 60s (Fig. 6C, S18). It is noteworthy that at most timepoints the bright LATp fluorescence spots could be observed. The lower medium temperature and cholesterol depletion by 1 mM mβCD resulted in delayed LATp phosphorylation and decreased clustering (Fig. S19, S20, correspondingly). Platelets activated by CRP exhibited the most significant increase in LATp phosphorylation after 300s (Fig. S21). The "CLEC-2 clustering" module parameter variation (k_1 and k_3 decrease and k_{-2} increase) allowed to accurately describe the decrease in LAT phosphorylation upon temperature lowering and cholesterol depletion (Fig. 6C, Table S15).

To investigate which part of the CLEC-2 signalling cascade is influenced by the temperature changes, we performed immunoblotting analysis of tyrosine phosphorylation level in platelets activated by fucoidan at room and body temperature (Fig. 6D-G). Washed human platelets at concentration 1.5 10^9/ml in modified Tyrode's buffer (no BSA and no Ca^{2+}) were incubated with fucoidan for 0-5m at given temperature conditions. Samples were taken at 15-30 s time intervals and analysed by immunoblotting with anti-phospho-tyrosine antibody PY20 as described in the Methods section. The analysis shows that while 1 μg/ml of fucoidan does not induce significant activation. On the other hand, both 10 and 100 μg/ml of fucoidan induced tyrosine phosphorylation with peak values at 90 s and 30 s respectively. The increase in temperature significantly shortened the lag-times of phosphorylation to 60 s and 15 s respectively. Thus we can conclude that the temperature variation influence activity of tyrosine kinases as well as calcium signalling. This result is in agreement with the model prediction that the rate of CLEC-2 clustering determines the time-lapse to peak platelet activation.

3.7. Impact of the medium temperature on CLEC-2 induced calcium response in single cells

TIRF-microscopy of immobilised single calcium-sensitive dye loaded platelets was performed, to investigate the nature of the cytosolic calcium increase observed in flow cytometry. We utilised two experimental settings. In the first setting, platelets were immobilised on VM64 (anti-CD31 clone (48)) antibody (Fig. 7A-D), and fucoidan solution in Tyrode's buffer was washed over the surface. Platelets developed cytosolic calcium spiking with varying intensity (Fig. 7A, C). Frequent cytosolic calcium spiking intensified by 50s after fucoidan addition (Fig. 7A-D). Maximal calcium concentration in the spikes, as well as spike frequency corresponded with the model predictions (Fig. 5A). Comparison between fucoidan-induced calcium spiking between 25°C (Fig. 7A) and 37°C (Fig. 7C) shows that the frequency of spiking increases at body temperature and there is also a noticable increase in amplitude. This result corresponds to the prediction that fucoidan-induced platelet activation could be influenced by the temperature-dependent parameters: receptor translocation and enzyme turnover rates. Together these data corroborate the model predictions that a) fucoidan induces calcium spiking in platelets and b) fucoidan-induced activation of platelets is significantly influenced by temperature. It could be noticed that while the amplitudes of the calcium spikes remained around the same values at different temperatures (Fig. 7F), the interspike time intervals were significantly shorter at 37°C than at 25°C (Fig. 7E). This observation corresponded with the model prediction that an increase in CLEC-2 clustering rates in the membrane lead to an increase in cytosolic calcium spiking (Fig. S22).

4. Discussion

Here we aimed at investigation of primary regulatory mechanisms of platelet CLEC-2 induced activation by means of comprehensive computational systems biology modelling. Our model accurately reproduced literature data on platelet activation by CLEC-2 agonists fucoidan, rhodocytin and podoplanin. The model gave a set of predictions. First, a rapid CLEC-2 clustering upon ligation was required for platelet activation by CLEC-2 agonists, which corresponded to data from (41) and our experiments with mβCD treated platelets (Fig. 5B). Second, CLEC-2 ligands are capable of inducing cytosolic calcium spiking independent on platelet secondary activation, which corresponded to data from (40) and our experiments with MRS2179 (Fig. 5A, 6A, B). Third, the sensitivity analysis of the model has revealed a key role of Syk kinases in the CLEC-2 signalling cascade (Fig. 3), which was in perfect agreement with (17, 56). Finally, the CLEC-2 clustering and LAT-signalosome formation appeared to be the rate-limiting steps in signal propagation in addition to tyrosine kinase activities. This proposition was supported by our experiments at different temperature conditions alongside different mβCD concentrations (Fig. 6, 7).

During model development, we applied mathematical equations from our previously published model of platelet aggregation (65) to describe the process of receptor clustering ("2-equation" model, Fig. S1B). The "2-equation" model described experimental data on CLEC-2 receptor clustering, as well as the computational results of a more conventional model of receptor clustering ("N-equation" model, Fig. S1A). Two possible receptor clustering patterns distinctive in the sequence of dimerisation and ligation of receptors were identified. However, only the inclusion of the pattern with rapid dimerisation in the model allowed it to reproduce experimentally observed calcium response (Fig. 3C, D). "The "Ligand-mediated receptor dimerisation" clustering pattern was in line with experimental data describing the capability of the CLEC-2 ligand to promote receptor clustering (35–37). Furthermore, this result was in agreement with previously published data on other ITAM-bearing receptors (41). On the other hand, CLEC-2 clustering upon activation by monomeric ligands (e.g. podoplanin) has been reported (38), which should correspond to "post-ligation" clustering, assuming conformational changes in the CLEC-2 structure upon ligation.

The analysis of the model predicted a central role of the Syk tyrosine kinase for CLEC-2 signalling cascade (Fig. 4A). This prediction corresponded to previously published data on CLEC-2 stimulation in platelets pre-treated with PRT-060318 (57) as well as CLEC-2 stimulation of platelets of mice deficient on

Syk activatory SH-2 domains (17). Sensitivity analysis has also revealed that, in addition to the tyrosine kinase activity, the PLCγ2 activity and receptor clustering, to a lesser extent, are the rate-limiting steps as well (Fig. 4). It is noteworthy that the parameters concerning dephosphorylation of signalling were as influential as the parameters concerning the activation of kinases (Fig. 4, S5). This result emphasises the role of the negative regulators of intracellular signalling for CLEC-2 induced platelet activation.

More accurate analysis of the parts of the platelet response influenced by the parameters revealed that, although the activity of tyrosine kinases had the most impact on every response, only CLEC-2 clustering influenced the time-lapse to peak concentration, while only moderately affecting the number of active signalling proteins. This observation was supported by the decrease in platelet activation time with temperature increase or mβCD supplementation (Fig. 6A, B). A similar effect could be expected from GPVI signalling, which also requires clustering of receptors. Indeed, when GPVI cluster formation was affected by losartan, a delay in platelet response to collagen appeared (66).

In order to test the model predictions that CLEC-2 clustering is one of the rate-limiting processes for the CLEC-2 signalling cascade, we investigated the influence of two membrane fluidity changing agents on platelet activation. First, we utilised incubation of platelets with a cholesterol-binding agent mβCD, which changes membrane cholesterol saturation and thus directly increases the fluidity of the membranes. We observed a faster platelet response to CLEC-2 agonists in the presence of mβCD (Fig. 5B, Fig. 6B). However, these results were in disagreement with previously published work (61), where CLEC-2 signalling was shown to be independent of lipid rafts, and lipid raft role was proposed mainly for secondary signalling. On the other hand, in (61) platelets were incubated with mβCD for an hour and this could have led to the reintroduction of cholesterol in the signalling region (67). The dose-dependent response to mβCD, obtained upon incubation for 15 minutes in our work (Fig. S3B) proves the membrane fluidity to be of significance for primary CLEC-2 response.

The second way to influence the rate of CLEC-2 clustering utilised here was a variation in the environment temperature. The temperature decrease from 37°C to 25°C resulted in a prolonged delay after activation (Fig. 6, Fig. 7). This result could not be considered as a direct confirmation of the receptor clustering impact, as it is well known that the temperature affects the turnover numbers of enzymes (68, 69) to the same degree as the rates of diffusion (70, 71). Experimental data on immunofluorescence microscopy additionally demonstrated impairment of LAT-signalosome formation upon temperature decrease and cholesterol depletion (Fig. 6C, Fig. S18-S20). Based on the model predictions, this is justified by the alterations in the receptor cluster formation at different conditions (Fig. 6C). Furthermore, the fact that the applied decrease in temperature did not affect the degree of activation is in agreement with the model prediction that the receptor clustering affects only the times of activation, while the tyrosine kinase activity controls both the time and the degree of activation (Fig. 4B-E, S8). Additionally, we demonstrated that such temperature variation has no significant effect on ADP-induced platelet activation, confirming the hypothesis that receptor clustering is specifically important for tyrosine kinase signalling (Fig. S17).

Among the main features of the model was its capability to work both in stochastic and in deterministic modes. Applicability of stochastic modelling to platelets is based on the fact that even at maximal degrees of activation upon CLEC-2 stimulation, amounts of crucial signalling proteins do not exceed 200 (Syk, LAT, PLCγ2).

Although the experimental data supported our model predictions, some limitations should be noted. While it has been shown that fucoidan is capable of activating platelet CLEC-2 (21), it has been demonstrated recently, that fucoidan might be activating GPVI and platelet endothelial aggregation receptor 1 (PEAR-1) as well (72, 73). However, PEAR-1 and GPVI participation in fucoidan induced platelet activation has been demonstrated by aggregometry (72), where the effects of secondary mediators of signalling are prevailing (34). Authors of (72) also report that fucoidan is not inducing

calcium signalling in platelets solely by implicating spectrofluorimetry, which is insensitive to weak calcium signalling.

The confirmations of model predictions here are limited to experiments with isolated platelets. A large part of the model predictions is concerned with kinase activity, not routinely assessed for single cells. For the experiments with immunoblotting, the distinction between primary and secondary signalling for tyrosine phosphorylation assays is not evident. Additional experiments on the roles of tyrosine kinases in CLEC-2 signalling as well as further model development (direct inclusion of the protein-tyrosine phosphatase 1B (PTP1B) phosphatase) and investigation of cooperativity between CLEC-2 and GPVI should be the subject of further studies.

The fact that the motion of proteins drives CLEC-2 activation in the plasma membrane and the assembly of signalling complexes demonstrated here allows us to take a new perspective on all receptors that perform clustering after activation or are associated with specific lipid micro-domains. The knowledge of the underlying mechanisms of receptor cluster assembly will push forward understanding of molecular signalling in all types of the eukaryotic cell as well as developing of new antithrombotic agents, specifically targeting receptor cluster formation.

References.

1. Versteeg, H.H., J.W.M. Heemskerk, M. Levi, and P.H. Reitsma. 2013. New fundamentals in hemostasis. *Physiol Rev.* 93:327–58.

2. van der Meijden, P.E.J., and J.W.M. Heemskerk. 2018. Platelet biology and functions: new concepts and clinical perspectives. *Nat. Rev. Cardiol.*

3. Repsold, L., R. Pool, M. Karodia, G. Tintinger, and A.M. Joubert. 2017. An overview of the role of platelets in angiogenesis, apoptosis and autophagy in chronic myeloid leukaemia. *Cancer Cell Int.* 17:1–12.

4. Nurden, A.T. 2007. Platelets and Tissue Remodeling: Extending the Role of the Blood Clotting System. *Endocrinology*. 148:3053–3055.

5. Gawaz, M., and S. Vogel. 2013. Platelets in tissue repair: control of apoptosis and interactions

with regenerative cells. *Blood*. 122:2550 LP – 2554.

6. Ed Rainger, G., M. Chimen, M.J. Harrison, C.M. Yates, P. Harrison, S.P. Watson, M. Lordkipanidzé, and G.B. Nash. 2015. The role of platelets in the recruitment of leukocytes during vascular disease. *Platelets*. 26:507–520.

7. Hitchcock, J.R., C.N. Cook, S. Bobat, E.A. Ross, A. Flores-Langarica, K.L. Lowe, M. Khan, C. Coral Dominguez-Medina, S. Lax, M. Carvalho-Gaspar, S. Hubscher, G. Ed Rainger, M. Cobbold, C.D. Buckley, T.J. Mitchell, A. Mitchell, N.D. Jones, N. Van Rooijen, D. Kirchhofer, I.R. Henderson, D.H. Adams, S.P. Watson, and A.F. Cunningham. 2015. Inflammation drives thrombosis after Salmonella infection via CLEC-2 on platelets. *J. Clin. Invest.* 125:4429–4446.

8. Watson, S.P., J.M.J. Herbert, and A.Y. Pollitt. 2010. GPVI and CLEC-2 in hemostasis and vascular integrity. *J. Thromb. Haemost.* 8:1456–67.

9. Stalker, T.J., D.K. Newman, P. Ma, K.M. Wannemacher, and L.F. Brass. 2012. Platelet signaling. *Handb. Exp. Pharmacol.* 59–85.

10. Gurbel, P.A., A. Kuliopulos, and U.S. Tantry. 2015. G-protein-coupled receptors signaling pathways in new antiplatelet drug development. *Arterioscler. Thromb. Vasc. Biol.* 35:500–512.

11. FitzGerald, G.A. 1991. Mechanisms of platelet activation: Thromboxane A_2 as an amplifying signal for other agonists. *Am. J. Cardiol.* 68:B11–B15.

12. Gibbins, J.M., M. Okuma, R. Farndale, M. Barnes, and S.P. Watson. 1997. Glycoprotein VI is the collagen receptor in platelets which underlies tyrosine phosphorylation of the Fc receptor γ-chain. *FEBS Lett.* 413:255–259.

13. Suzuki-Inoue, K., Y. Kato, O. Inoue, K.K. Mika, K. Mishima, Y. Yatomi, Y. Yamazaki, H. Narimatsu, and Y. Ozaki. 2007. Involvement of the snake toxin receptor CLEC-2, in podoplanin-mediated platelet activation, by cancer cells. *J. Biol. Chem.* 282:25993–26001.

14. Christou, C.M., A.C. Pearce, A. a Watson, A.R. Mistry, A.Y. Pollitt, A.E. Fenton-May, L.A. Johnson, D.G. Jackson, S.P. Watson, and C. a O'Callaghan. 2008. Renal cells activate the platelet receptor CLEC-2 through podoplanin. *Biochem J*. 411:133–140.

15. Bertozzi, C.C., A.A. Schmaier, P. Mericko, P.R. Hess, Z. Zou, M. Chen, C.Y. Chen, B. Xu, M.M. Lu, D. Zhou, E. Sebzda, M.T. Santore, D.J. Merianos, M. Stadtfeld, A.W. Flake, T. Graf, R. Skoda, J.S. Maltzman, G.A. Koretzky, and M.L. Kahn. 2010. Platelets regulate lymphatic vascular development through CLEC-2-SLP-76 signaling. *Blood*. 116:661–670.

16. Suzuki-Inoue, K., O. Inoue, G. Ding, S. Nishimura, K. Hokamura, K. Eto, H. Kashiwagi, Y. Tomiyama, Y. Yatomi, K. Umemura, Y. Shin, M. Hirashima, and Y. Ozaki. 2010. Essential in vivo roles of the C-type lectin receptor CLEC-2: Embryonic/neonatal lethality of CLEC-2-deficient mice by blood/lymphatic misconnections and impaired thrombus formation of CLEC-2-deficient platelets. *J. Biol. Chem.* 285:24494–24507.

17. Hughes, C.E., B.A. Finney, F. Koentgen, K.L. Lowe, and S.P. Watson. 2015. The N-terminal SH2 domain of Syk is required for (hem) ITAM , but not integrin , signaling in mouse platelets. *Blood*. 125:144–155.

18. Herzog, B.H., J. Fu, S.J. Wilson, P.R. Hess, A. Sen, J.M. McDaniel, Y. Pan, M. Sheng, T. Yago, R. Silasi-Mansat, S. McGee, F. May, B. Nieswandt, A.J. Morris, F. Lupu, S.R. Coughlin, R.P. McEver, H. Chen, M.L. Kahn, and L. Xia. 2013. Podoplanin maintains high endothelial venule integrity by interacting with platelet CLEC-2. *Nature*. 502:105–109.

19. Huang, T.F., C.Z. Liu, and S.H. Yang. 1995. Aggretin, a novel platelet-aggregation inducer from snake (Calloselasma rhodostoma) venom, activates phospholipase C by acting as a glycoprotein Ia/IIa agonist. *Biochem. J.* 309:1021–7.

20. Shin, Y., and T. Morita. 1998. Rhodocytin, a functional novel platelet agonist belonging to the heterodimeric C-type lectin family, induces platelet aggregation independently of glycoprotein Ib. *Biochem Biophys Res Commun*. 245:741–745.

21. Manne, B.K., T.M. Getz, C.E. Hughes, O. Alshehri, C. Dangelmaier, U.P. Naik, S.P. Watson, and S.P. Kunapuli. 2013. Fucoidan is a novel platelet agonist for the C-type lectin-like receptor 2 (CLEC-2). *J. Biol. Chem.* 288:7717–7726.

22. Boulaftali, Y., P.R. Hess, T.M. Getz, A. Cholka, M. Stolla, N. Mackman, A.P. Owens, J. Ware, M.L. Kahn, and W. Bergmeier. 2013. Platelet ITAM signaling is critical for vascular integrity in infammation. *J. Clin. Invest.* 123:908–916.

23. Hughes, C.E., L. Navarro-Nunez, B.A. Finney, D. Mour??o-S??, A.Y. Pollitt, and S.P. Watson. 2010. CLEC-2 is not required for platelet aggregation at arteriolar shear. *J. Thromb. Haemost.* 8:2328–2332.

24. Bender, M., F. May, V. Lorenz, I. Thielmann, I. Hagedorn, B.A. Finney, T. Vögtle, K. Remer, A. Braun, M. Bösl, S.P. Watson, and B. Nieswandt. 2013. Combined in vivo depletion of glycoprotein VI and C-type lectin-like receptor 2 severely compromises hemostasis and abrogates arterial thrombosis in mice. *Arterioscler. Thromb. Vasc. Biol.* 33:926–934.

25. Gros, A., V. Syvannarath, L. Lamrani, V. Ollivier, S. Loyau, T. Goerge, B. Nieswandt, M. Jandrot-Perrus, and B. Ho-Tin-Noé. 2015. Single platelets seal neutrophil-induced vascular breaches via GPVI during immune-complex-mediated inflammation in mice. *Blood*. 126:1017–1026.

26. May, F., I. Hagedorn, I. Pleines, M. Bender, T. Vogtle, J. Eble, M. Elvers, and B. Nieswandt. 2009. CLEC-2 is an essential platelet activating receptor in hemostasis and thrombosis. *Blood*. 114:3464–3473.

27. Inoue, O., K. Hokamura, T. Shirai, M. Osada, N. Tsukiji, K. Hatakeyama, K. Umemura, Y. Asada, K. Suzuki-Inoue, and Y. Ozaki. 2015. Vascular smooth muscle cells stimulate platelets and facilitate thrombus formation through platelet CLEC-2: Implications in atherothrombosis. *PLoS One*. 10:1–28.

28. Pike, L.J. 2009. The challenge of lipid rafts. *J. Lipid Res.* 50:S323–S328.

29. Payne, H., T. Ponomaryov, S.P. Watson, and A. Brill. 2017. Mice with a deficiency in CLEC-2 are protected against deep vein thrombosis. *Blood*. 129:2013–2020.

30. Shirai, T., O. Inoue, S. Tamura, N. Tsukiji, T. Sasaki, H. Endo, K. Satoh, M. Osada, H. Sato-Uchida, H. Fujii, Y. Ozaki, and K. Suzuki-Inoue. 2017. C-type lectin-like receptor 2 promotes hematogenous tumor metastasis and prothrombotic state in tumor-bearing mice. *J. Thromb. Haemost.* 15:513–525.

31. Kato, Y., M.K. Kaneko, A. Kunita, H. Ito, A. Kameyama, S. Ogasawara, N. Matsuura, Y. Hasegawa, K. Suzuki-inoue, O. Inoue, Y. Ozaki, and H. Narimatsu. 2008. Molecular analysis of the pathophysiological binding of the platelet aggregation-inducing factor podoplanin to the C-type lectin-like receptor CLEC-2. *Cancer Sci.* 99:54–61.

32. O'Rafferty, C., G.M. O'Regan, A.D. Irvine, and O.P. Smith. 2015. Recent advances in the pathobiology and management of Kasabach-Merritt phenomenon. *Br. J. Haematol.* 171:38–51.

33. Chang, Y.-W., P. Hsieh, Y. Chang, M. Lu, T.-F. Huang, K.-Y. Chong, H.-R. Liao, J.-C. Cheng, and C.-P. Tseng. 2015. Identification of a novel platelet antagonist that binds to CLEC-2 and suppresses podoplanin-induced platelet aggregation and cancer metastasis. *Oncotarget*. 6:42733–48.

34. Pollitt, A.Y., B. Grygielska, B. Leblond, L. Désiré, J.A. Eble, and S.P. Watson. 2010. Phosphorylation of CLEC-2 is dependent on lipid rafts, actin polymerization, secondary mediators, and Rac. *Blood*. 115:2938–2946.

35. Watson, A.A., C.M. Christou, J.R. James, A.E. Fenton-May, G.E. Moncayo, A.R. Mistry, S.J. Davis, R.J.C. Gilbert, A. Chakera, and C.A. O'Callaghan. 2009. The platelet receptor CLEC-2 is active as a dimer. *Biochemistry*. 48:10988–10996.

36. Hughes, C.E., A.Y. Pollitt, J. Mori, J.A. Eble, M.G. Tomlinson, J.H. Hartwig, C.A. O'Callaghan, K. Fütterer, and S.P. Watson. 2010. CLEC-2 activates Syk through dimerization. *Blood*. 115:2947–2955.

37. Watson, A.A., J.A. Eble, and C.A. O'Callaghan. 2008. Crystal structure of rhodocytin, a ligand for the platelet-activating receptor CLEC-2. *Protein Sci.* 17:1611–6.

38. Pollitt, A.Y., N.S. Poulter, E. Gitz, L. Navarro-Nuñez, Y.J. Wang, C.E. Hughes, S.G. Thomas, B. Nieswandt, M.R. Douglas, D.M. Owen, D.G. Jackson, M.L. Dustin, and S.P. Watson. 2014. Syk and src family kinases regulate c-type lectin receptor 2 (clec-2)-mediated clustering of podoplanin and platelet adhesion to lymphatic endothelial cells. *J. Biol. Chem.* 289:35695–35710.

39. Inoue, K., Y. Ozaki, K. Satoh, Y. Wu, Y. Yatomi, Y. Shin, and T. Morita. 1999. Signal transduction pathways mediated by glycoprotein Ia/IIa in human platelets: Comparison with those of glycoprotein VI. *Biochem. Biophys. Res. Commun.* 256:114–120.

40. Badolia, R., V. Inamdar, B.K. Manne, C. Dangelmaier, J.A. Eble, and S.P. Kunapuli. 2017. Gq pathway regulates proximal C-type lectin-like receptor-2 (CLEC-2) signaling in platelets. *J. Biol. Chem.* 292:14516–14531.

41. Mukherjee, S., J. Zhu, J. Zikherman, R. Parameswaran, T.A. Kadlecek, Q. Wang, B. Au-Yeung, H. Ploegh, J. Kuriyan, J. Das, and A. Weiss. 2013. Monovalent and Multivalent Ligation of the B Cell Receptor Exhibit Differential Dependence upon Syk and Src Family Kinases. *Sci. Signal.* 6:ra1 LP-ra1.

42. Poulter, N.S., A.Y. Pollitt, D.M. Owen, E.E. Gardiner, R.K. Andrews, H. Shimizu, D. Ishikawa, D. Bihan, R.W. Farndale, M. Moroi, S.P. Watson, and S.M. Jung. 2017. Clustering of glycoprotein VI (GPVI) dimers upon adhesion to collagen as a mechanism to regulate GPVI signaling in platelets. *J. Thromb. Haemost.* 15:549–564.

43. Dunster, J.L., A.J. Unsworth, A.P. Bye, E.J. Haining, M.A. Sowa, Y. Di, T. Sage, C. Pallini, J.A. Pike, A.T. Hardy, B. Nieswandt, Á. García, S.P. Watson, N.S. Poulter, J.M. Gibbins, and A.Y. Pollitt. 2020. Interspecies differences in protein expression do not impact the spatiotemporal regulation of glycoprotein VI mediated activation. *J. Thromb. Haemost.* 18:485–496.

44. Dunster, J.L., F. Mazet, M.J. Fry, J.M. Gibbins, and M.J. Tindall. 2015. Regulation of Early Steps of GPVI Signal Transduction by Phosphatases: A Systems Biology Approach. *PLoS Comput. Biol.* 11:1–26.

45. Sveshnikova, A.N., A. V. Balatskiy, A.S. Demianova, T.O. Shepelyuk, S.S. Shakhidzhanov, M.N. Balatskaya, A. V. Pichugin, F.I. Ataullakhanov, and M.A. Panteleev. 2016. Systems biology insights into the meaning of the platelet's dual-receptor thrombin signaling. *J. Thromb. Haemost.* 14:2045–2057.

46. Gillespie, D.T. 2007. Stochastic simulation of chemical kinetics . *Annu. Rev. Phys. Chem.* 58:35–55.

47. Dunster, J.L., M.A. Panteleev, J.M. Gibbins, and A.N. Sveshnikova. 2018. Mathematical Techniques for Understanding Platelet Regulation and the Development of New Pharmacological Approaches. . pp. 255–279.

48. Mazurov, A. V, D. V Vinogradov, N. V Kabaeva, G.N. Antonova, Y.A. Romanov, T.N. Vlasik, A.S. Antonov, and V.N. Smirnov. 1991. A monoclonal antibody, VM64, reacts with a 130 kDa glycoprotein common to platelets and endothelial cells: heterogeneity in antibody binding to human aortic endothelial cells. *Thromb. Haemost.* 66:494—499.

49. Panteleev, M.A., N.M. Ananyeva, N.J. Greco, F.I. Ataullakhanov, and E.L. Saenko. 2005. Two subpopulations of thrombin-activated platelets differ in their binding of the components of the intrinsic factor X-activating complex. *J.Thromb.Haemost.* 3:2545–2553.

50. Gibbins, J.M. 2004. Study of Tyrosine Kinases and Protein Tyrosine Phosphorylation BT - Platelets and Megakaryocytes: Volume 2: Perspectives and Techniques. In: Gibbins JM, MP Mahaut-Smith, editors. . Totowa, NJ: Humana Press. pp. 153–167.

51. Mahammad, S., and I. Parmryd. 2015. Cholesterol Depletion Using Methyl-β-cyclodextrin. In: Owen DM, editor. Methods in Membrane Lipids. New York, NY: Springer New York. pp. 91–102.

52. Lawrence, M.B., L. V McIntire, and S.G. Eskin. 1987. Effect of flow on polymorphonuclear leukocyte/endothelial cell adhesion. *Blood*. 70:1284 LP – 1290.

53. Pahle, J. 2009. Biochemical simulations: Stochastic, approximate stochastic and hybrid approaches. *Brief. Bioinform.* 10:53–64.

54. Gillespie, D.T. 2007. Stochastic Simulation of Chemical Kinetics. *Annu. Rev. Phys. Chem.* 58:35–55.

55. Balabin, F.A., and A.N. Sveshnikova. 2016. Computational biology analysis of platelet signaling reveals roles of feedbacks through phospholipase C and inositol 1,4,5-trisphosphate 3-kinase in controlling amplitude and duration of calcium oscillations. *Math. Biosci.* 276:67–74.

56. Severin, S., A.Y. Pollitt, L. Navarro-Nunez, C.A. Nash, D. Mour??o-S??, J.A. Eble, Y.A. Senis, and S.P. Watson. 2011. Syk-dependent phosphorylation of CLEC-2: A novel mechanism of hem-immunoreceptor tyrosine-based activation motif signaling. *J. Biol. Chem.* 286:4107–4116.

57. Manne, B.K., R. Badolia, C. Dangelmaier, J.A. Eble, W. Ellmeier, M. Kahn, and S.P. Kunapuli. 2015. Distinct pathways regulate Syk protein activation downstream of immune tyrosine activation motif (ITAM) and hemITAM receptors in platelets. *J. Biol. Chem.* 290:11557–11568.

58. Fuller, G.L.J., J.A.E. Williams, M.G. Tomlinson, J.A. Eble, S.L. Hanna, S. Pöhlmann, K. Suzuki-Inoue, Y. Ozaki, S.P. Watson, and A.C. Pearce. 2007. The C-type lectin receptors CLEC-2 and Dectin-1, but not DC-SIGN, signal via a novel YXXL-dependent signaling cascade. *J. Biol. Chem.* 282.

59. Bradshaw, J.M. 2010. The Src, Syk, and Tec family kinases: Distinct types of molecular switches. *Cell. Signal.* 22:1175–1184.

60. Tsang, E., A.M. Giannetti, D. Shaw, M. Dinh, J.K.Y. Tse, S. Gandhi, A. Ho, S. Wang, E. Papp, and J.M. Bradshaw. 2008. Molecular mechanism of the Syk activation switch. *J. Biol. Chem.* 283:32650–32659.

61. Manne, B.K., R. Badolia, C.A. Dangelmaier, and S.P. Kunapuli. 2015. C-type lectin like receptor 2 (CLEC-2) signals independently of lipid raft microdomains in platelets. *Biochem. Pharmacol.* 93:163–170.

62. Baba, Y., and T. Kurosaki. 2011. Impact of Ca2+ signaling on B cell function. *Trends Immunol.* 32:589–594.

63. Sveshnikova, A.N., F.I. Ataullakhanov, and M.A. Panteleev. 2015. Compartmentalized calcium signaling triggers subpopulation formation upon platelet activation through PAR1. *Mol. Biosyst.* 11:1052–1060.

64. Burkhart, J.M., M. Vaudel, S. Gambaryan, S. Radau, U. Walter, L. Martens, J. Geiger, A. Sickmann, and R.P. Zahedi. 2012. The first comprehensive and quantitative analysis of human platelet protein composition allows the comparative analysis of structural and functional pathways. *Blood*. 120.

65. Filkova, A.A.A.A., A.A.A.A. Martyanov, M.A. Garzon Dasgupta, A.K. Panteleev, A.N.A.N. Sveshnikova, A.K. Garzon Dasgupta, M.A. Panteleev, and A.N.A.N. Sveshnikova. 2019.

Quantitative dynamics of reversible platelet aggregation: mathematical modelling and experiments. *Sci. Rep.* 9:6217.

66. Jiang, P., S. Loyau, M. Tchitchinadze, J. Ropers, G. Jondeau, and M. Jandrot-Perrus. 2015. Inhibition of Glycoprotein VI Clustering by Collagen as a Mechanism of Inhibiting Collagen-Induced Platelet Responses: The Example of Losartan. *PLoS One*. 10:e0128744.

67. Mahammad, S., and I. Parmryd. 2015. Cholesterol Depletion Using Methyl-β-cyclodextrin. In: Owen DM, editor. Methods in Membrane Lipids. New York, NY: Springer New York. pp. 91–102.

68. Robinson, P.K. 2015. Enzymes: principles and biotechnological applications. *Essays Biochem.* 59:1–41.

69. Struvay, C., and G. Feller. 2012. Optimization to low temperature activity in psychrophilic enzymes. *Int. J. Mol. Sci.* 13:11643–11665.

70. Medda, L., M. Monduzzi, and A. Salis. 2015. The molecular motion of bovine serum albumin under physiological conditions is ion specific. *Chem. Commun.* 51:6663–6666.

71. Saha, S., I.-H. Lee, A. Polley, J.T. Groves, M. Rao, and S. Mayor. 2015. Diffusion of GPI-anchored proteins is influenced by the activity of dynamic cortical actin. *Mol. Biol. Cell*. 26:4033–4045.

72. Kardeby, C., K. Fälker, E.J. Haining, M. Criel, M. Lindkvist, R. Barroso, P. Påhlsson, L.U. Ljungberg, M. Tengdelius, G.E. Rainger, S. Watson, J.A. Eble, M.F. Hoylaerts, J. Emsley, P. Konradsson, S.P. Watson, Y. Sun, and M. Grenegård. 2019. Synthetic glycopolymers and natural fucoidans cause human platelet aggregation via PEAR1 and GPIbα. *Blood Adv.* 3:275–287.

73. Alshehri, O.M., S. Montague, S. Watson, P. Carter, N. Sarker, B.K. Manne, J.L.C. Miller, A.B. Herr, A.Y. Pollitt, C.A.O. Callaghan, S. Kunapuli, C.E. Hughes, and S.P. Watson. 2015. Activation of glycoprotein VI (GPVI) and C-type lectin-like receptor-2 (CLEC-2) underlies platelet activation by diesel exhaust particles and other charged / hydrophobic ligands. 2:459–473.

Figure legends

Figure 1. CLEC-2 induced signalling in blood platelets. In resting platelets, relatively few Syk kinases are active due to low SFK activity. Upon ligation of the platelet CLEC-2, and CLEC-2 cluster formation, tyrosine residues in the CLEC-2 cytoplasmic domain (YxxL sequence, hemITAM) become phosphorylated by Syk kinases. Non-active Syk bind to phosphorylated hemITAM with its SH2 domains and become active via trans-autophosphorylation. Accumulation of the active Syk results in downstream platelet activation and calcium signalling.

Figure 2. Scheme of the model of platelet CLEC-2 signalling. "CLEC-2 clustering" module (A): after CLEC-2 ligation CLEC-2 molecules to formed clusters. Model of the CLEC-2 clustering is based on (65). Activated CLEC-2 molecules could form CLEC-2 clusters, which could form larger clusters by binding single activated CLEC-2 molecules or other clusters. Clusters decayed into cluster and cluster or cluster and single CLEC-2 molecule. "Quiescent state" module (B): active CD148 produces 1/3 active SFK, which are negatively regulated by active Csk. 1/3 active SFK auto-phosphorylated and became 2/3 active SFK. Active CD148 negatively regulated this reaction. All forms of active SFK mediated CD148, Csk and Syk activation. Active Syk activated non-active Syk. "Tyrosine kinase" module (C): after cluster formation, active Syk phosphorylated hemITAM in the CLEC-2 cytoplasmic domains. Inactive Syk or 2/3 active SFK bound phospho-hemITAMs (two for Syk and one for SFK) with their SH2 domains and became active. Active Syk also mediated TULA-2 phosphatase activation, which is a negative regulator of Syk activity. "LAT-PLCγ2" module (D): active Syk phosphorylated the adaptor protein LAT. PLCγ2 and PI3K bound P-LAT, which activated PI3K. Active PI3K phosphorylated PIP_2 and produced PIP_3, which became a docking site for Btk. Btk activated upon PIP_3 binding and activated PLCγ2. Active PLCγ2 hydrolysed PIP_2 and produced IP_3. "Calcium" module (D): IP_3 activated IP3R on the surface of the DTS. Through active IP3R free Ca^{2+} ions passed to the cytosol. Ca^{2+} inhibited

IP3R as well and returned to the DTS via SERCA. Dark blue lines represented transitions between species; light blue lines represent catalysis. Copy numbers of active Syk (E), LAT (F) and PLCγ2 (G) were fitted to experimental data on fucoidan induced platelet activation from (21).

Figure 3. Comparison of the receptor clustering patterns effects on platelet CLEC-2 induced activation. Two patterns of receptor clustering – ligand-mediated receptor clustering (rapid receptor dimerisation upon ligation – black) and post-ligation clustering (ligation does not lead to rapid receptor dimerisation – red) - A. Both approaches resulted in cytosolic calcium spiking. However, post-ligation model resulted in a significantly delayed activation in comparison to rapid-dimerisation model (C). Averaging of the calcium concentration over 500 stochastic runs of the model also demonstrated that delayed model demonstrated significantly delayed, but yet amplified response in comparison to rapid-dimerisation model (D).

Figure 4. Sensitivity analysis and variation of the unknown parameters. Sensitivity scores for the effect of parameter variation on the concentration of active PLCγ2 were calculated (A). Explicit variation of the parameters with the highest sensitivity scores for the effect on maximal PLCγ2 number and time to reach maximum: CLEC-2 clustering k_{-2} (B), CLEC-2 clustering k_{-1} (C), CLEC-2 clustering k_3 (D), CLEC-2 initial number (E), turnover rate of Syk kinases (F), Michaelis constant of Syk kinases (G), forward rate of Syk activation upon SH-2 domain binding to dually phosphorylated hemITAMs (H), Syk initial number (I), reverse rate of LAT phosphorylation (J), turnover rate of Btk (K), Michaelis constant of Btk (L), LAT initial number (M).

Figure 5. CLEC-2-evoked calcium signalling in platelets. Continuous flow cytometry analysis of highly diluted platelet suspension (1×10^3 plt/ml) revealed that CLEC-2 agonist fucoidan induced calcium response is independent of the presence of MRS2179 (A) while being gradually dependent on the concentration of mβCD (B). Single-cell analysis using TIRF-microscopy revealed that platelets are capable of spreading on fucoidan-covered glass (C) and that immobilised fucoidan is capable of evoking calcium oscillations in platelets (D).

Figure 6. Platelet CLEC-2 signalling is dependent on temperature conditions. Flow cytometry assay of CLEC-2 induced signalling in platelets after activation by 100 µg/ml of fucoidan. Activation at 25°C was significantly slower than at 37°C (A). Disruption of lipid rafts by mβCD delayed activation (B). Each curve represents data from at least three experiments. (C) Comparison of the immunofluorescent assays with computational model predictions describing the dependence of platelet CLEC-2 induced activation from medium temperature and cholesterol presence in the cell membrane. Each experimental time-point is averaged over 50 platelets. (D-G) Immunoblot assay of CLEC-2 induced signalling (D – raw data): platelets were activated by 1(E)-10(G)-100(F) µg/ml of fucoidan at 25°C or 37°C. Samples for analysis were taken 0-15-30-60-90-120-150-180-300 s after activation. Murine anti-human-phosphotyrosine primary anti-bodies (PY-20 clone) were used. Anti-tubulin primary antibodies were used as loading control after stripping. A typical experiment for one out of n = 3 different donors.

Figure 7. Cytosolic calcium spiking induced by fucoidan in single cells. Platelets were loaded with Fura-2, immobilised on VM-64 (A-D) and then illuminated by 405 nm laser. Cytosolic calcium concentration was recalculated from Fura-2 fluorescence (see Methods). Washed platelets were immobilised on VM64 antibody (A-D). At time-point "0" fucoidan solution at 100 µg/ml was added. Cytosolic calcium spiking (A, C) and whole-cell fluorescence (B, D) were monitored at room temperature (A, B) or 37 $^{\circ}$C (C, D). Representative curves out of n=10. I, J – Intervals between calcium spikes (E) and calcium concentration per spike (F), spread on VM-64 and activated by fucoidan at 25°C (black) or 37°C (red). Data collected from 20 cells.